

Regular Article

Low Molecular Weight Branched PEI Binding to Linear DNA

Kuniharu Utsuno,^{*,a} Hiroyuki Kono,^a Emika Tanaka,^a Nozomi Jouna,^a Yohichiro Kojima,^b and Hasan Uludağ^{*,c,d,e}

^aDepartment of Science & Engineering for Materials, National Institute of Technology, Tomakomai College; Tomakomai, Hokkaido 059–1275, Japan; ^bDepartment of Electrical & Electronic Engineering, Hokkaido University of Science; Sapporo 006–8585, Japan; ^cDepartment of Chemical & Materials Engineering, University of Alberta; Edmonton, AB T6G 2V2, Canada; ^dDepartment of Biomedical Engineering, University of Alberta; Edmonton, AB T6G 2V2, Canada; and ^eFaculty of Pharmacy & Pharmaceutical Sciences, University of Alberta; Edmonton, AB T6G 2V2, Canada.

Received June 6, 2016; accepted June 26, 2016

Polyethylenimine (PEI) is one of the most versatile non-viral vectors used in gene therapy, especially for delivering plasmid DNA to human cells. However, a good understanding of PEI binding to DNA, the fundamental basis for the functioning of PEI as a vector, has been missing in the literature. In this study, PEI (branched, 600 Da) binding to DNA was examined by isothermal titration calorimetry (ITC), quartz crystal microbalance (QCM) and a complementary set of analysis tools. We demonstrated that a separation between the binding heat and the condensation heat is needed and that the excluded site model should be used for PEI binding stage in the ITC analysis. The equilibrium constant for PEI binding to DNA was determined to be $2.5 \times 10^5 \text{ M}^{-1}$ from the ITC analysis, and as $2.3 \times 10^5 \text{ M}^{-1}$ from the QCM analysis. Additionally, we suggested that the 600 Da branched PEI binds to the major groove of DNA and the rearrangement of PEI on DNA may be difficult to occur because of the small dissociation rate. The binding analysis presented here can be employed to improve our understanding of the functioning of PEI and PEI-like non-viral vectors.

Key words DNA condensation; polyethylenimine; isothermal titration calorimetry; quartz crystal microbalance; thermodynamics; kinetics

The cationic polyelectrolyte polyethylenimine (PEI) is one of the most versatile polymers used for non-viral gene delivery.^{1–3)} PEI binds to DNA via electrostatic interactions between the positively charged PEI amine groups and the negatively charged nucleic acid phosphate groups in the DNA backbone. PEI, by neutralizing the DNA molecule, facilitates its condensation into particles in the ‘nano-meter’ range.⁴⁾ It is believed that PEI’s strong transfection ability is due to its effective ability to condense the DNA molecule into a nanoparticle,^{5–7)} which facilitates its cellular uptake and subsequent intracellular trafficking. PEI is available in a broad range of molecular weights. Higher molecular weight PEIs have high transfection efficiency, but lead to excessive cytotoxicity. Low molecular weight PEIs have demonstrated low toxicity on cells, but they also display low transfection efficiency.⁵⁾ Recently, highly efficient non-viral vectors have been developed by modifying low molecular weight (600 Da) PEI with a variety of functional groups.^{8–12)}

To better understand PEI interactions with the DNA molecule, we previously determined the thermodynamic parameters of PEI binding to DNA using isothermal titration calorimetry (ITC).¹³⁾ In that study, two types of binding modes were found to describe the interactions between PEI and DNA. One type of binding involves PEI binding to the DNA groove, another likely binding mode involves external binding of PEI to the DNA phosphate backbone. Recently, Ketola *et al.* showed that the equilibrium constant of 25 kDa branched PEI to plasmid DNA (7164 bp) using time-resolved fluorescence spectroscopy was $7.3 \times 10^3 \text{ M}^{-1}$ under the buffer conditions of 50 mM maximal electroschock seizure or 2-(*N*-morpholino)ethanesulfonic acid (buffer) (MES), 50 mM *N*-(2-

hydroxyethyl)piperazine-*N'*-2-ethanesulfonic acid (HEPES) and 75 mM sodium chloride (NaCl) (pH 7.4).¹⁴⁾ This value is slightly lower than the value obtained from our previous study under similar ionic and pH conditions ($1.0\text{--}1.8 \times 10^4 \text{ M}^{-1}$ under 0.1 M NaCl).¹³⁾ In contrast, Smith *et al.* reported that the equilibrium constant of 25 kDa linear PEI binding to plasmid DNA (3546 bp) was $7.6 \times 10^8 \text{ M}^{-1}$ under 10 mM HEPES (pH 7.4) based on ITC measurements.¹⁵⁾ This equilibrium constant is 760 times larger than the one obtained from our previous result under similar 10 mM HEPES (pH 7.0) condition ($1 \times 10^6 \text{ M}^{-1}$).¹³⁾ The observed difference may be due to the difference in the mass and architecture of the PEI used, since 600 Da branched PEI was used in our study¹³⁾ while 25 kDa linear PEI was used in the Smith *et al.* study.¹⁵⁾ Another possibility for the difference in the reported equilibrium constant may come from the fitting model used for analysis. We used the model developed by Kim *et al.*,¹⁶⁾ while Smith *et al.* used the standard multiple site model.¹⁵⁾ It was difficult to analyze the ITC data in these studies since not only PEI gets protonated when it binds to DNA, but also the DNA is condensed during the binding process,¹³⁾ which complicates the interpretation of the released (absorbed) heat during the titration process. Therefore, a more comprehensive analysis of PEI–DNA interactions would be beneficial to better understand the underlying basis of PEIs’ effectiveness in DNA delivery.

In this study, we performed ITC measurements of PEI binding to DNA in the TAE buffer (which contains ethylenediaminetetraacetic acid (EDTA) and typically used in gel electrophoresis of DNA) in order to minimize the protonation of PEI during the titration process. We applied excluded site model proposed by Velázquez-Campoy (which was based on

*To whom correspondence should be addressed. e-mail: utsuno@tomakomai-ct.ac.jp; huludag@ualberta.ca

McGhee and von Hippel theory) for fitting of ITC data since the use of single set of identified site (SSIS) model (also Kim's model) overestimate the equilibrium constant.^{17–19)} To obtain an independent assessment of the fitting model used to analyze the ITC data, we additionally determined the equilibrium constant of PEI binding to DNA using quartz crystal microbalance (QCM). QCM is a sensitive method that facilitates the kinetic assessment of biomolecular interactions,²⁰⁾ where a host molecule is immobilized on the quartz surface and then the analyte is injected. When the analyte molecule is captured by the host molecule, the mass of the oscillator increases, resulting in a decrease in the frequency of oscillation. The change in oscillation frequency is proportional to mass adsorbed to the sensor surface, enabling quantitative determination of adsorption. We obtained the binding kinetics of DNA to PEI from the time courses of frequency decreases and calculated the equilibrium constant from the DNA concentration dependence of the binding kinetics. Finally, fluorescent displacement assays were performed to determine the binding mode of PEI to DNA. Fluorescent displacement assays reveal DNA affinity through decreased fluorescence of the dye as it is displaced from its binding state on DNA to free in solution, as PEI comes in contact with DNA–dye complex.¹⁵⁾ This is a commonly used assay for characterizing polyplex formation for non-viral gene delivery agents. By using two fluorophores whose DNA binding mode is well established, we probed the location of the bound PEI on the DNA strand. In this way, our collective results provided a more comprehensive understanding of PEI binding to the DNA molecule.

Experimental

¹³C-NMR Spectroscopy Twenty milligram per milliliters solutions of 600Da branched PEI (with 14 Ns; Polysciences, Warrington, PA, U.S.A.) or EDTA (Dojindo Laboratories, Kumamoto, Japan) were prepared by dissolving in a mixture of 90% (v/v) D₂O and 10% (v/v) H₂O, and then the pH of the solutions was adjusted to pH=8.2 by addition of 1N HCl or NaOH. The PEI+EDTA solution (10mg/mL) was prepared by mixing both solutions equally. Each solution was placed in 5mm NMR tube (Wako Pure Chemical Industries, Ltd., Osaka, Japan). ¹³C-NMR spectra were recorded on an AVIII NMR spectrometer (Bruker BioSpin GmbH, Germany, 500.13 MHz for ¹H and 125.13 MHz for ¹³C) equipped with a 2-channel 5mm broad band observe probe incorporating a z-gradient coil. The measurement temperature was set to 298 K. ¹³C-chemical shifts were calibrated by assigning the methyl peak of 4,4-dimethyl-4-silapentane-1-sulfonic acid as 0ppm.

ITC Analysis The PEI and salmon testes DNA (Sigma, St. Louis, MO, U.S.A.) were separately dissolved in TAE buffer (40mM Tris–acetic acid, 1mM EDTA, pH 8.2). For direct titration, 1.4mM DNA solution (phosphate concentration) was applied into the ITC cell (950μL; Nano-ITC from TA Instruments Inc., New Castle, DE, U.S.A.) and 20mM PEI solution (nitrogen concentration) in the 250μL syringe was injected into the DNA solution in 20 portions of 12.5μL at 4- or 30-min intervals. The syringe was stirred 250rpm and the cell was equilibrated at 25.0°C. The 20mM PEI solution was also injected into the TAE buffer as a blank titration. For reverse titration, 1mM PEI solution was applied into the cell and 3.9mM DNA solution in syringe was injected into the PEI solution. Each experiment was carried out 4 times (2 times of

4-min interval and 2 times of 30-min interval).

ITC Model Fitting To describe binding, we used the model proposed by Kim *et al.* since it is highly flexible for the two-variable equilibrium constant system.¹⁶⁾ Briefly, their model is based on the SSIS model.²¹⁾ The equation of the SSIS model is:

$$Q = \frac{nM_t\Delta HV_0}{2} \left[1 + \frac{X_t}{nM_t} + \frac{1}{nKM_t} - \sqrt{\left(1 + \frac{X_t}{nM_t} + \frac{1}{nKM_t} \right)^2 - \left(\frac{4X_t}{nM_t} \right)} \right] \quad (1)$$

where Q is the total heat content of the solution contained in the sample cell, n is the stoichiometric number, M_t is the total concentration of DNA, X_t is the total concentration of PEI, ΔH is the molar heat of the PEI binding, V_0 is the cell volume and K is the equilibrium constant. The heat released $\Delta Q(i)$ from the i th injection (injected volume: V_i) is given by:

$$\Delta Q(i) = Q(i) + \frac{dV_i}{V_0} \left[\frac{Q(i) + Q(i-1)}{2} \right] - Q(i-1) \quad (2)$$

The normalized heat, NDH(i), is calculated by dividing the $\Delta Q(i)$ with the number of moles in the i th injected volume. In the model proposed by Kim *et al.*, the fraction of bound PEIs is described as the absolute value of NDH divided by ΔH . NDH1 is the heat of first binding stage, which is determined by ΔH_1 , K_1 , and n_1 . NDH2 is the heat of the second binding stage, which is determined by ΔH_2 , K_2 , and n_2 . To calculate n_2 the fitting parameters n'_2 and n_3 are used.

We also used the model proposed by Velázquez-Campoy, which is based on excluded site model.¹⁹⁾ In this model, the heat effect associated with injection, $\Delta Q(i)$, was defined as follows:

$$\begin{aligned} \Delta Q(i) = V_0 & \left(\Delta H \left(M_{t,i}v_{\text{isol},i} - \left(1 - \frac{dV_i}{V_0} \right) M_{t,i-1}v_{\text{isol},i-1} \right) \right. \\ & + \left(\Delta H + \frac{\Delta h}{2} \right) \left(M_{t,i}v_{\text{sc},i} - \left(1 - \frac{dV_i}{V_0} \right) M_{t,i-1}v_{\text{sc},i-1} \right) \\ & \left. + (\Delta H + \Delta h) \left(M_{t,i}v_{\text{dc},i} - \left(1 - \frac{dV_i}{V_0} \right) M_{t,i-1}v_{\text{dc},i-1} \right) \right) \end{aligned} \quad (3)$$

where Δh is the enthalpy associated with the interaction between nearest neighbor bound ligands and v_{isol} , v_{sc} , and v_{dc} are the partial numbers of ligand molecules bound isolated, with only one nearest neighbor (singly contiguous) and with two nearest neighbors (doubly contiguous), per macromolecule, respectively.

$$v_{\text{isol}} = (X_t - M_t v) \frac{L - lv}{K_d} \left(\frac{(2\omega - 1)(L - lv) + v - R}{2(\omega - 1)(L - lv)} \right)^{l+1} \quad (4)$$

$$\begin{aligned} v_{\text{sc}} = (X_t - M_t v) & \frac{\omega}{\omega - 1} \frac{(l - 1)v - L + R}{K_d} \\ & \times \left(\frac{(2\omega - 1)(L - lv) + v - R}{2(\omega - 1)(L - lv)} \right)^l \end{aligned} \quad (5)$$

$$v_{dc} = (X_t - M_t v) \left(\frac{\omega}{2(\omega - 1)} \right)^2 \frac{((l - 1)v - L + R)^2}{K_d(L - lv)} \times \left(\frac{(2\omega - 1)(L - lv) + v - R}{2(\omega - 1)(L - lv)} \right)^{l-1} \quad (6)$$

where L is the number of nucleotides per DNA molecule, l is the number of nucleotides occupied by a PEI molecule, K_d is a dissociation constant, ω is a cooperativity parameter,

$$R = ((L - (l + 1)v)^2 + 4\omega v(L - lv))^{1/2} \quad (7)$$

and v is the number of PEI molecules bound per DNA molecule.

$$v = v_{\text{isol}} + v_{\text{sc}} + v_{\text{dc}} \quad (8)$$

Electrophoretic Mobility Shift Assay (EMSA) The samples for gel mobility shift assay were prepared similar to the samples in the ITC direct titration experiment. The PEI and DNA were dissolved in TAE buffer. A 12.5 μL of 20 mM PEI solution was added into 950 μL of 1.4 mM DNA solution. After mixing, 12.5 μL of solution was removed for analysis with 0.5% agarose gel electrophoresis. The addition of 20 mM PEI solution and the extraction from the solution for EMSA analysis were repeated 20 times. Gel electrophoresis was performed in TAE buffer at 120 V for 30 min.

QCM Analysis An AFFINIX QN μ (Initium, Kanagawa, Japan) QCM instrument was used, with a 27-MHz QCM

plate.^{22–24} The gold electrode was cleaned with 1% sodium dodecyl sulfate (SDS) and piranha solution (3 parts H_2SO_4 :1 part 30% H_2O_2) before PEI immobilization. The gold electrode of the QCM plate was soaked into 1 mM 3,3'-dithiodipropionic acid (DTDPA) solution at room temperature overnight. The carboxylic acid of DTDPA on the QCM was reacted with *N*-hydroxysuccinimide in the presence of 1-ethyl-3-(3-dimethylaminopropyl) carbodiimide for 20 min. The QCM having the activated carboxyl groups was immersed in 450 μL of water. Then, 50 μL of 0.4 M PEI was added and the frequency decrease was equilibrated at about 300 Hz. The QCM was immersed into 50 mM ethanolamine for 10 min to deactivate the carboxyl group. The sensor cell containing the immobilized PEI was immersed in 450 μL of TAE buffer, then 50 μL of DNA solution was injected. The time course of frequency changes was measured at 25.0°C.

Fluorescent Dye Displacement Assay Fluorescent dye displacement measurements were performed using RF-540 spectrofluorometer (Shimadzu, Kyoto, Japan) to obtain fluorescence intensities. The relative intensity was calculated using the following equation:

$$\text{Relative intensity} = (F_{\text{obs}} - F_0) / (F_{\text{DNA}} - F_0) \quad (9)$$

where F_{obs} , F_0 , and F_{DNA} are the fluorescence intensities of a given sample, the dye in buffer alone, and the dye complexed to DNA alone, respectively.²⁵ The fluorescence intensity was measured under condition of 30 μM DNA in TAE buffer containing 0.20 μM ethidium bromide (EtBr) (excitation 518 nm,

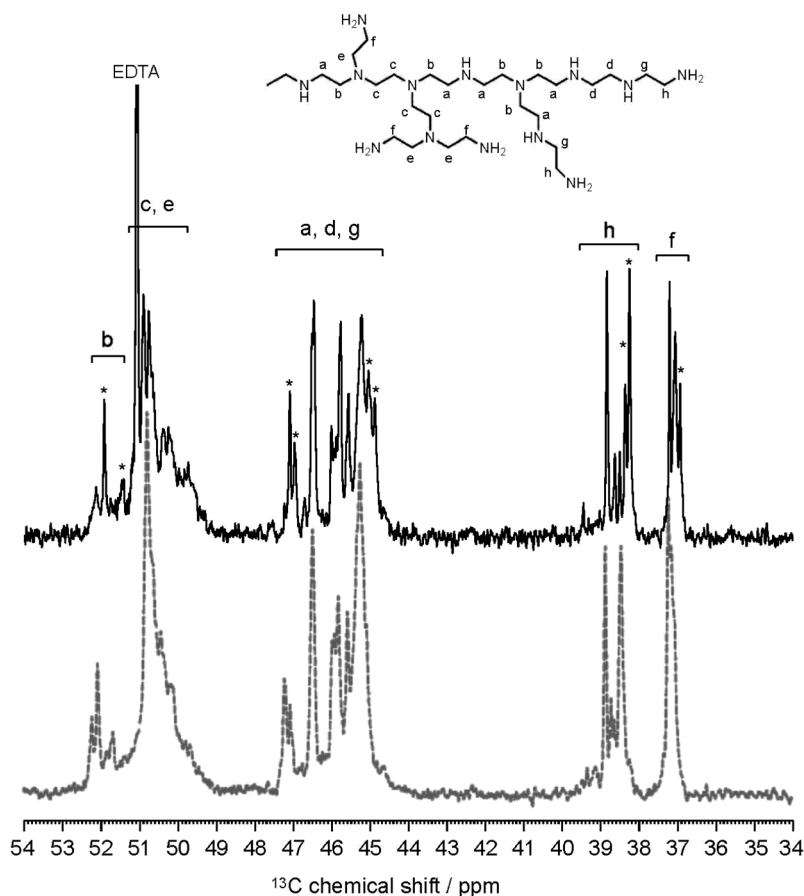


Fig. 1. ^{13}C -NMR Spectra of PEI in the Presence (Solid Line) and Absence (Dashed Line) of EDTA Dissolved in a Mixture of 90% D_2O and 10% H_2O

emission 585 nm), or Hoechst 33258 (excitation 358 nm, emission 446 nm) at room temperature ($25 \pm 2^\circ\text{C}$). PEI solution was added to the DNA solution so that it became the same N/P ratio as the ITC study and the measurements were repeated.

Light Scattering Measurements Total intensity light scattering was performed by using the same spectrofluorometer as dye displacement assay. The excitation and emission monochromators were set to 480 nm, and the scattered light was measured at 90° angle with respect to the incident beam.²⁶⁾ PEI solution was added to $30 \mu\text{M}$ DNA in TAE buffer at room temperature ($25 \pm 2^\circ\text{C}$) so that it became the same N/P ratio as the ITC study and the measurements were repeated.

Results

Protonation of PEI in the Presence of EDTA ^{13}C -NMR spectra of the PEI in the presence and absence of EDTA were shown in Fig. 1. As shown in the figure, there are eight types of methylene carbon atoms (a–g) in PEI structure, and the chemical shifts for these carbons were recently assigned by Holycross and Chai.²⁷⁾ Multiplicity of the ^{13}C resonances for

the same methylene carbons are due to various sizes, oligomers, and impurities of PEI. As indicated by the asterisks on the spectrum of PEI with EDTA, many methylene carbon resonances were shifted to upfield about 0.1–0.25 ppm by EDTA. These upfield shifts caused by EDTA is related to protonation of amino groups in the PEI; N atom in the amino groups has unpaired electrons, and thus the methylene carbons next to the amino groups are shielded by the N atom. When the N atom is protonated by Hs from EDTA, the shielding effect to the vicinal carbon atom is diminished or weakened, resulting in upfield shift of the methylene carbon atom. Therefore, the protonation of amino groups in the PEI caused by EDTA was considered the reason for the slight upfield-shift for select methylene carbons.

Characterization of PEI–DNA Binding from ITC

Figure 2a shows the raw data of heat release for direct titration of DNA with PEI from the ITC. After the first 8 endothermic peaks, exothermic peaks appeared (solid line) in the case of PEI–DNA titration, whereas, all peaks were exothermic in the case of blank titration (dotted line). The reproducibility of 4 independent experiments was very good. Figure 2b shows the result of the EMSA. The samples from the sixth to ninth titration showed retardation, which corresponded to the endothermic–exothermic transition region in the ITC data. In the case of reverse titration (DNA addition to PEI), the first 11 peaks were endothermic (Fig. 2c) and the remaining peaks were exothermic.

The integrated data for the heat released at each titration is shown in Fig. 3. The thermodynamic parameters for the titration were obtained using a SSIS model.²¹⁾ The number of

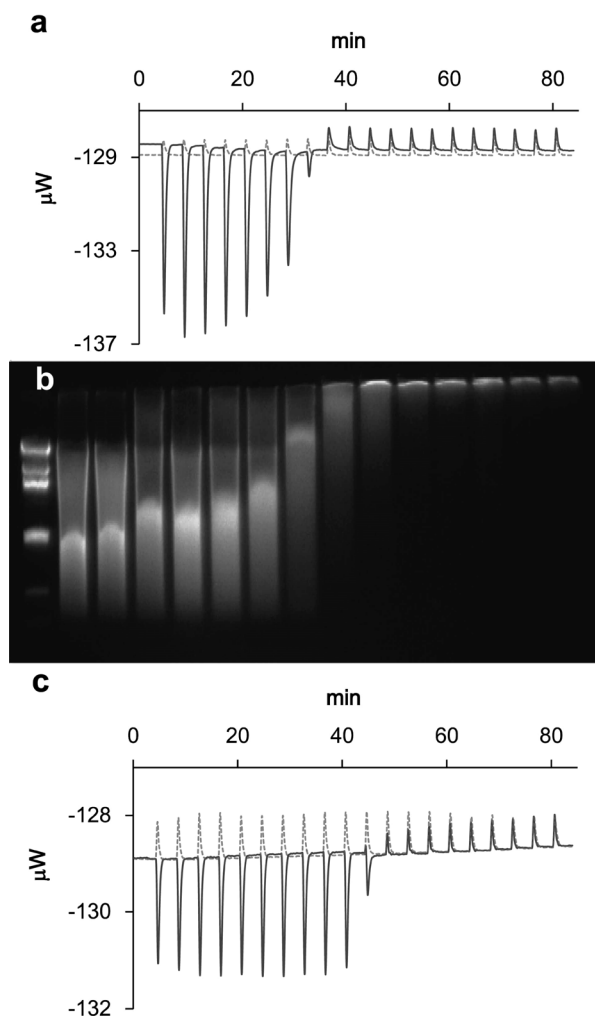


Fig. 2. (a) Calorimetric Thermograms for Titration of 20 mM PEI into 1.4 mM DNA (Solid Line) and into Buffer (Dotted Line); (b) Gel Mobility Shift Assay; Left to Right: λ -HindIII Marker, DNA Only, PEI–DNA Complexes Equivalent to 1st to 13th Titration of 20 mM PEI into 1.4 mM DNA; (c) Calorimetric Thermograms for the Titration of 3.9 mM DNA into 1 mM PEI (Solid Line) and into Buffer (Dotted Line)

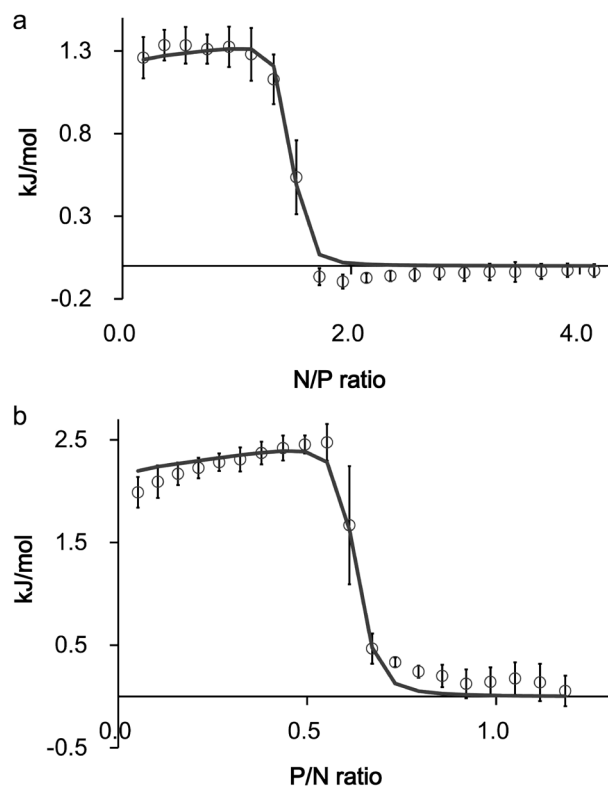


Fig. 3. Integrated ITC Curves Fitted with SSIS Model

(a) Direct titration. Fitting parameters were: $n=1.4$, $K=3.5 \times 10^5 \text{ M}^{-1}$, and $\Delta H=1.3 \text{ kJ/mol}$. (b) Reverse titration. Fitting parameters were: $n^*=0.6$, $K=1.2 \times 10^6 \text{ M}^{-1}$, and $\Delta H^*=2.2 \text{ kJ/mol}$.

PEI nitrogens binding to a DNA phosphate (n) was 1.4, the equilibrium constant (K) was $3.5 \times 10^5 \text{ M}^{-1}$, and the enthalpy change (ΔH) for 1 mol of PEI nitrogen binding to DNA was 1.3 kJ/mol (Fig. 3a). In the reverse titration, on the other hand, the number of DNA phosphate binding to a PEI nitrogen (n^*) was 0.6, the equilibrium constant was $1.2 \times 10^6 \text{ M}^{-1}$, and the enthalpy change (ΔH^*) for 1 mol of DNA phosphate binding to PEI was 2.2 kJ/mol (Fig. 3b). The n was 1.7 derived from n^* by reciprocal transformation, and ΔH was 1.3 kJ/mol to multiplied ΔH^* by 0.6. A significant difference between actual and fitted data was apparent around the transition region of acute change of heat.

As the SSIS model corresponded poorly with the experimental data especially at the transition points, we postulated the existence of a second site for PEI binding. We used the model proposed by Kim *et al.* because it is not restricted by the assumption $K_1 > K_2$.¹⁶⁾ Figure 4 shows the integrated ITC curve fitted with the Kim's model. NDH2 which shows dashed line is the heat of second binding stage. The obtained values (Table 1) for first binding stage resemble those derived from the SSIS model, except for K_1 value of direct titration.

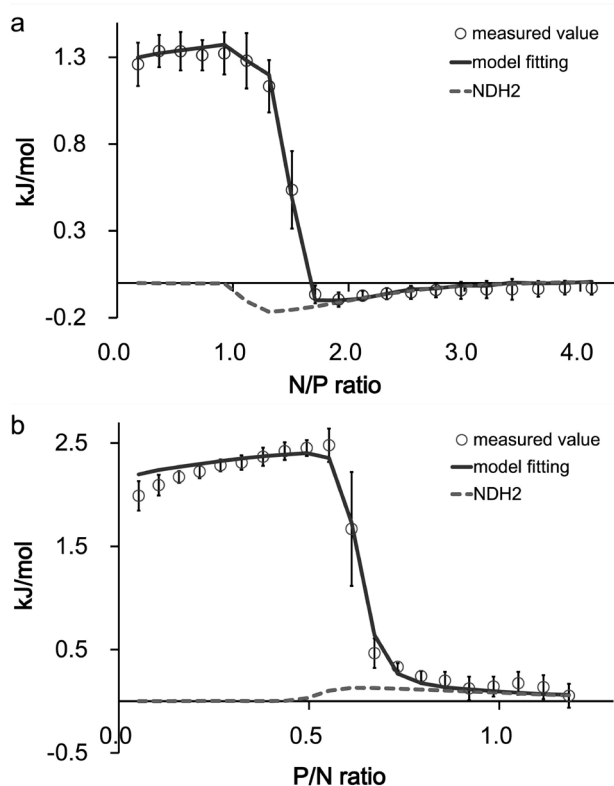


Fig. 4. Integrated ITC Curves Fitted with Kim's Model
(a) Direct titration. (b) Reverse titration. The heat of the second binding stage (NDH2) is shown by dashed line.

$$n_1 = 1.4, K_1 = 1.0 \times 10^6 \text{ M}^{-1}, \Delta H_1 = 1.3 \text{ kJ/mol for direct titration}$$

$$n_1^* = 0.6, K_1^* = 1.0 \times 10^6 \text{ M}^{-1}, \Delta H_1^* = 2.2 \text{ kJ/mol for reverse titration}$$

Interestingly, we got the parameters $\Delta H_2 = -0.2 \text{ kJ/mol}$, $K_2 = 7000 \text{ M}^{-1}$, $n_3 = 1.0$, $n'_2 = 2.0$ for direct titration, $\Delta H_2^* = 0.2 \text{ kJ/mol}$, $K_2^* = 7000 \text{ M}^{-1}$, $n_3^* = 0.5$ (correspond to n'_2 of direct titration), $n'_2 = 1.0$ (correspond to n_3 of direct titration) for reverse titration. The second binding stage is likely to correlate with the DNA condensation because ΔH_2 and ΔH_2^* absolute values were same but the sign was converse. The ΔG was calculated from $\Delta G = -RT \ln K$, which gave a ΔG for second binding stage of -22 kJ/mol .

According to McGhee-von Hippel, Scatchard representation, on which SSIS model is based, has a serious defect in numerating the number of free sites along the polymer lattice.¹⁷⁾ We employed the model proposed by Velázquez-Campoy to fit the first binding stage¹⁹⁾ since the use of SSIS model (Scatchard representation) overestimate the equilibrium constant.¹⁸⁾ The model is based on the McGhee-von Hippel formalism modified for the analysis of ITC. Before model fitting, we subtracted the NHD2 (heat of second binding stage) from the observed data. Figure 5 shows the subtracted data fitted

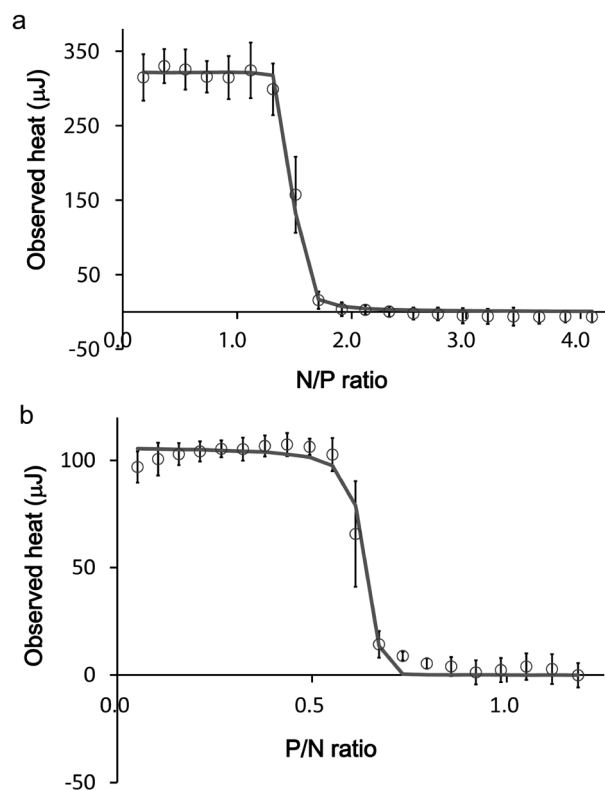


Fig. 5. Subtracted ITC Data Fitted with the Model Proposed by Velázquez-Campoy
(a) Direct titration. (b) Reverse titration.

Table 1. Fitting Parameters for the Model Proposed by Kim *et al.*

	ΔH_1 (kJ/mol)	K_1 (M^{-1})	n_1	n_3	ΔH_2 (kJ/mol)	K_2 (M^{-1})	n'_2	n_2 ($n'_2 - n_3$)
Direct	1.3	1000000	1.4	1.0	-0.2	7000	2.0	1.0
Reverse	2.2	1000000	0.6	0.5	0.2	7000	1.0	0.5

The errors are within 10%.

with the model proposed by Velázquez-Campoy. The same fitting parameters were used between direct and reverse titration data except l (the number of nucleotides occupied by a PEI molecule). The number of nucleotides per DNA molecule (L) was set as 4000 bases from the result of gel electrophoresis (Fig. 2b). A 600Da PEI molecule contains 14 nitrogen atoms. The dissociation constant (K_d) was $1.0 \times 10^{-9} \text{ M}$, the cooperativity parameter (ω) was 0.999, the enthalpy for 1 mol of PEI molecule binding to DNA ($\Delta H_{\text{molecule}}$) was 18 kJ, the enthalpy associated with the interaction between nearest neighbor bound ligands (ΔH) was 0. The number of nucleotides occupied by a PEI molecule (l) was 9.5 for the direct titration and 8.0 for the reverse titration. The values obtained from this fitting were transformed to the counterparts to N/P ratio system using following equations:

$$n = \frac{\text{the number of nitrogen atoms contained in a PEI molecule}}{l} \quad (10)$$

$$K = (L \times K_d)^{-1} \quad (11)$$

$$\Delta H = \frac{\Delta H_{\text{molecule}}}{\text{the number of nitrogen atoms contained in a PEI molecule}} \quad (12)$$

The equilibrium constant (K) was calculated to be $2.5 \times 10^5 \text{ M}^{-1}$, and the enthalpy change (ΔH) for 1 mol of PEI nitrogen binding to DNA was 1.3 kJ/mol, the number of PEI nitrogens binding to a DNA phosphate (n) was 1.5 for the direct titration, 1.8 for the reverse titration (Table 2).

Equilibrium Constant from QCM The binding kinetics of DNA to PEI was calculated from the time courses of frequency decreases in QCM.²⁴ The frequency change observed was proportional to the quantity of DNA bound to PEI (Δm of Eq. 14). In Eq. 14, k_{obs} is an observed association rate constant which is expressed as a function of total DNA concentration (Eq. 15). In Eq. 15, k_1 is an association rate constant and k_{-1} is a dissociation rate constant.



$$\Delta m_t = \Delta m_{\text{max}} \{1 - \exp(-k_{\text{obs}} \times t)\} \quad (14)$$

$$k_{\text{obs}} = k_1[\text{DNA}] + k_{-1} \quad (15)$$

Δm_t is the quantity of DNA which bind to the PEI immobilized in QCM cell at t seconds. Δm_{max} is the maximum

Table 2. Thermodynamic Parameters for First Binding Stage Obtained from Different Models

	ΔH_1 (kJ/mol)	K_1 (M^{-1})	n_1
SSIS (Direct)	1.3	350000	1.4
SSIS (Reverse)	1.3	1200000	1.7
Kim's (Direct)	1.3	1000000	1.4
Kim's (Reverse)	1.3	1000000	1.7
Excluded site (Direct)	1.3	250000	1.5
Excluded site (Reverse)	1.3	250000	1.8

The parameters from reverse titration were converted to comparable values to the parameters from direct titration. The parameters obtained from excluded site model were transformed to the counterparts to N/P ratio system. The errors are within 10%.

amount of DNA which bind to the PEI immobilized in QCM cell at equilibrium.

Figure 6a shows the frequency decrease when 50 μL of 0.92 mM DNA solution was injected in PEI-immobilized QCM cell which was immersed in 450 μL of TAE buffer. The frequency declined rapidly for the first 50 s after which the slope become gradually zero. The frequency is viewed as nearly-constant after 100 s.

Figure 6b shows the plots of the k_{obs} against DNA concentration, with a linear least-squares method applied to fit the data. According to Eq. 15, k_1 is derived from the slope of line and the value of k_{-1} corresponds to the ordinate intercept in Fig. 6b. The QCM analysis yielded values for k_1 of $0.32 \times 10^3 \text{ s}^{-1} \text{ M}^{-1}$ and k_{-1} of $1.4 \times 10^{-3} \text{ s}^{-1}$. The equilibrium constant (K) can be calculated by dividing k_1 by k_{-1} , giving K of $2.3 \times 10^5 \text{ M}^{-1}$.

Characterization of PEI Binding to DNA by Dye Displacement and Light Scattering Figure 7 shows the results of dye displacement assays. When DNA is pre-equilibrated with EtBr, ca. 70% of the EtBr is displaced upon PEI addition. On the other hand, when DNA is pre-equilibrated with Hoechst 33258, ca. 20% of the Hoechst 33258 is eventually displaced upon PEI addition. It appears that the displacement of both dyes are similar in early stages of titration (*i.e.*, N/P ratio <1) but eventually a different fraction of each dye remains bound to the DNA in the presence of PEI.

Figure 8 shows the plots of scattered light intensity of DNA solution when adding PEI in normal titration. The scattering is markedly increased after the N/P=1. This N/P ratio corresponds to the value that the second binding stage begins in

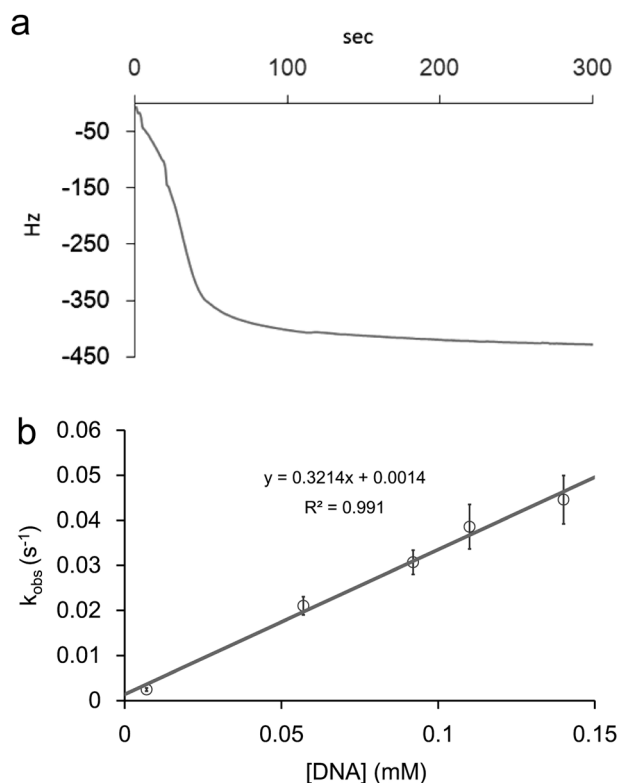


Fig. 6. (a) The Frequency Decrease When 50 μL of 0.92 mM DNA Solution was Injected in PEI-Immobilized QCM Cell Which Contains 450 μL of TAE Buffer; (b) The Plot of the k_{obs} against DNA Concentration

The data points (mean \pm S.D.) are independent triplicate measurements.

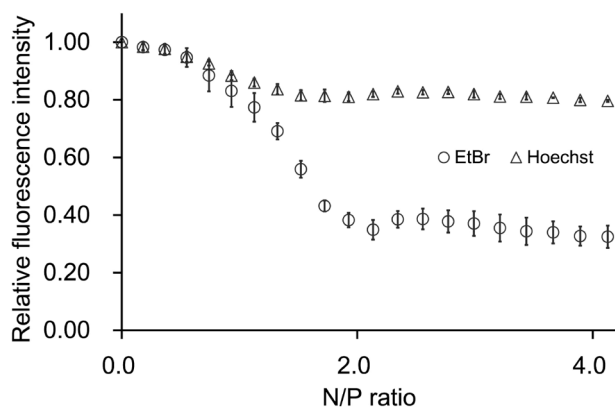


Fig. 7. Results of Dye Displacement Assays by Using Ethidium Bromide (EtBr) and Hoechst 33258

The data points (mean \pm S.D.) are triplicate measurements.

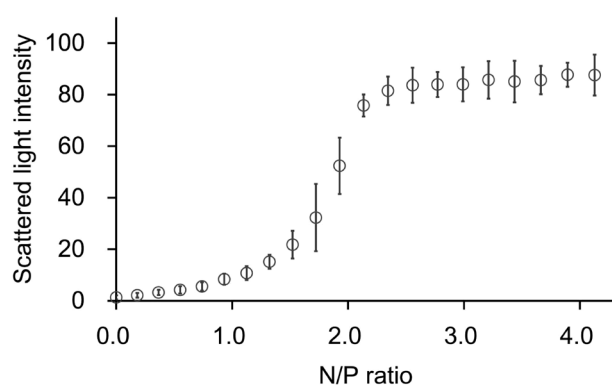


Fig. 8. Plots of Scattered Light Intensity of DNA Solution after Adding PEI

The data points are the mean \pm S.D. of 6 measurements.

Kim's model fitting of the ITC data (see Fig. 4). This confirms that the second binding stage corresponds to DNA condensation.

Discussion and Conclusion

The n obtained from reverse titration differs with the one from direct titration (PEI to DNA). When $[DNA] \ll [PEI]$, PEI molecules bind adjacently on DNA lattice. On the other hand, PEI molecules locate far from each other on DNA when $[DNA] \gg [PEI]$. Consequently, the gaps unavailable for the binding of PEI are increased. The rearrangement of PEI on DNA may be difficult to occur because k_{-1} is small. The equilibrium constant obtained from the QCM measurements ($2.3 \times 10^5 M^{-1}$) is very similar to the equilibrium constant obtained from the ITC ($2.5 \times 10^5 M^{-1}$), hence validating the excluded site model used to fit our ITC data.

Following the displacement of fluorescent probes during titrations has been a well utilized approach to understand the nature of binding between a ligand and DNA. Whereas EtBr interact with DNA by intercalating between the bases along the double helix,^{18,28} Hoechst 33258 binds in the minor groove of the DNA preferentially.²⁹ Based on the displacement of these well-established fluorophores, most of the PEI binds to the DNA region other than minor groove, since the fluorescence intensity decrease with Hoechst was only 20% after PEI binding. Considering that PEI pushes out the majority of EtBr,

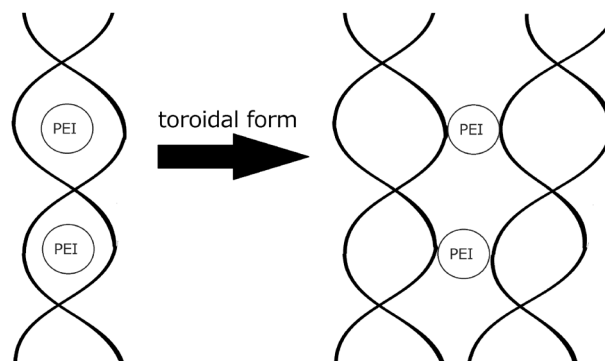


Fig. 9. The Schematic View about the DNA Condensation

PEI is pulled out from the groove to the phosphate of DNA backbone when adjacent DNAs get closer and toroidal structure is formed.

which intercalates between the DNA base pairs, we conclude that PEI should be located in DNA major groove. It was interesting to note that a similar decrease in fluorescence levels were observed for the two probes at the beginning of titration ($N/P < 1$); this was indicative of a more broad (indiscriminate) PEI binding pattern at the beginning of titrations where the DNA was in an extended configuration. Since condensation is observed, and expected to occur (from light scattering measurements) after this critical ratio ($N/P = 1.1$), it appears that PEI binding becomes more selective after the onset of condensation, showing a preference to the DNA major groove.

According to Wu *et al.*, Cobalt hexamine locate in the minor groove of DNA at low concentration while it binds the major groove of DNA at high concentration.³⁰ The 600 Da PEI may behave in a similar way as cobalt hexamine to form the ion-bridge configuration between adjacent B-DNAs. A small increase in fluorescence levels at $N/P = 2.3$ implicates that PEI is pulled out from the groove to the phosphate of DNA backbone when adjacent DNAs get closer and toroidal structure is formed (Fig. 9).

The binding of other PEI-like cationic molecules was investigated in independent studies. For example, Ruiz-Chica *et al.* reported putrescine, spermidine and spermine binding to DNA using Raman spectroscopy; whereas the former two polyamines were proposed to show a preferential binding to DNA minor groove, binding of the largest polyamine spermine was hypothesized to occur at the major groove of DNA.³¹ Considering that our PEI (*ca.* 600 Da) is even larger than spermine (*ca.* 202 Da), it is not surprising that PEI would have interacted with the less sterically-hindered major groove. Similarly, Vijayanathan *et al.* reported that spermine-like polyamines were stabilized in the major groove of DNA.²⁶ Our molecular dynamics studies also showed that a 600 Da branched PEI binds to 4 base pairs in the major groove of DNA.³² This corresponds to $l=8$, which was the parameter used in excluded site model in this study.

A negative ΔH of DNA condensation reaction was observed in our previous study (Fig. 2c and Table 1 in ref. 13), but the value was 4.4 times larger than one in this study. The reason for this could be the higher ionic strength in this study as compared to our previous study. According to Matulis *et al.*, the ΔH for DNA condensation by cobalt hexamine decreases with the increment of salt concentration.³³ Since the ΔG is -22 kJ per 1 mol nitrogen of PEI and a 600 Da PEI contains 14 nitrogens, the ΔG for a PEI molecule is -308 kJ. This value

is approximately 10 times larger than the one for spermidine obtained by Matulis *et al.*

We conducted the same ITC experiments using 25 kDa PEI instead of 600 Da PEI. However, we could not obtain reliable results because the observed data varied widely. This implicates that the large PEI could bind to DNA multivalently, while the small PEI could bind monovalently.

In conclusion, we demonstrated that the separation between the binding heat and the condensation heat is needed and that the excluded site model should be used for PEI binding stage in the ITC analysis. To avoid the protonation heat when PEI binds to DNA, PEI was protonated in the presence of EDTA (see Fig. 1). In consequence, more reliable model fitting of ITC data was attained. We further showed that QCM result supports the validity of ITC model fittings. The equilibrium constant was determined to be $2.5 \times 10^5 \text{ M}^{-1}$ from the ITC analysis, and $2.3 \times 10^5 \text{ M}^{-1}$ from the QCM analysis, providing a good consistency between the two independent methods. Additionally, we suggest that the rearrangement of PEI on DNA may be difficult to occur because the dissociation rate constant is small.

Acknowledgments This work was supported in part by Grants-in-Aid for Scientific Research C-25410134 from the Japan Society for Promotion of Science (H.K.). The ITC instrument used in this study were purchased through a Grant from Natural Sciences and Engineering Council of Canada (NSERC). Operating funds were provided by an NSERC Discovery Grant.

Conflict of Interest The authors declare no conflict of interest.

References

- 1) Boussif O., Lezoualc'h F., Zanta M. A., Mergny M. D., Scherman D., Demeneix B., Behr J.-P., *Proc. Natl. Acad. Sci. U.S.A.*, **92**, 7297–7301 (1995).
- 2) Neuberg P., Kichler A., *Adv. Genet.*, **88**, 263–288 (2014).
- 3) Godbey W. T., Wu K. K., Mikos A. G., *J. Control. Release*, **60**, 149–160 (1999).
- 4) Dunlap D. D., Maggi A., Soria M. R., Monaco L., *Nucleic Acids Res.*, **25**, 3095–3101 (1997).
- 5) Neu M., Fischer D., Kissel T., *J. Gene Med.*, **7**, 992–1009 (2005).
- 6) Banerjee P., Reichardt W., Weissleder R., Bogdanov A. Jr., *Bioconj. Chem.*, **15**, 960–968 (2004).
- 7) Godbey W. T., Wu K. K., Hirasaki G. J., Mikos A. G., *Gene Ther.*, **6**, 1380–1388 (1999).
- 8) Zhao J., Yang L., Huang P., Wang Z., Tan Y., Liu H., Pan J., He C.-Y., Chen Z.-Y., *J. Colloid Interface Sci.*, **463**, 93–98 (2016).
- 9) Li J.-M., Wang Y.-Y., Zhang W., Su H., Ji L.-N., Mao Z.-W., *Int. J. Nanomedicine*, **8**, 2101–2117 (2013).
- 10) Zhao F., Yin H., Zhang Z., Li J., *Biomacromolecules*, **14**, 476–484 (2013).
- 11) Huang H., Yu H., Tang G., Wang Q., Li J., *Biomaterials*, **31**, 1830–1838 (2010).
- 12) Yao H., Ng S. S., Tucker W. O., Tsang Y.-K.-T., Man K., Wang X.-m., Chow B. K. C., Kung H.-F., Tang G.-P., Lin M. C., *Biomaterials*, **30**, 5793–5803 (2009).
- 13) Utsuno K., Uludağ H., *Biophys. J.*, **99**, 201–207 (2010).
- 14) Ketola T.-M., Hanzlíková M., Leppänen L., Raviña M., Bishop C. J., Green J. J., Urtti A., Lemmetyinen H., Yliperttula M., Vuorimaa-Laukkanen E., *J. Phys. Chem. B*, **117**, 10405–10413 (2013).
- 15) Smith R. J., Beck R. W., Prevett L. E., *Biophys. Chem.*, **203–204**, 12–21 (2015).
- 16) Kim W., Yamasaki Y., Kataoka K., *J. Phys. Chem. B*, **110**, 10919–10925 (2006).
- 17) McGhee J. D., von Hippel P. H., *J. Mol. Biol.*, **86**, 469–489 (1974).
- 18) Utsuno K., Tsuboi M., *Chem. Pharm. Bull.*, **45**, 1551–1557 (1997).
- 19) Velázquez-Campoy A., *Anal. Biochem.*, **348**, 94–104 (2006).
- 20) Arnau A., *Sensors*, **8**, 370–411 (2008).
- 21) Freire E., Mayorga O. L., Straume M., *Anal. Chem.*, **62**, 950A–959A (1990).
- 22) Mori T., Toyoda M., Ohtsuka T., Okahata Y., *Anal. Biochem.*, **395**, 211–216 (2009).
- 23) Takahashi S., Matsuno H., Furusawa H., Okahata Y., *Anal. Biochem.*, **361**, 210–217 (2007).
- 24) Okahata Y., Niikura K., Sugiura Y., Sawada M., Morii T., *Biochemistry*, **37**, 5666–5672 (1998).
- 25) Wiethoff C. M., Gill M. L., Koe G. S., Koe J. G., Middaugh C. R., *J. Pharm. Sci.*, **92**, 1272–1285 (2003).
- 26) Vijayanathan V., Lyall J., Thomas T., Shirahata A., Thomas T. J., *Biomacromolecules*, **6**, 1097–1103 (2005).
- 27) Holycross D. R., Chai M., *Macromolecules*, **46**, 6891–6897 (2013).
- 28) Utsuno K., Tsuboi M., Katsumata S., Iwamoto T., *Chem. Pharm. Bull.*, **49**, 413–417 (2001).
- 29) Utsuno K., Maeda Y., Tsuboi M., *Chem. Pharm. Bull.*, **47**, 1363–1368 (1999).
- 30) Wu Y.-Y., Zhang Z.-L., Zhang J.-S., Zhu X.-L., Tan Z.-J., *Nucleic Acids Res.*, **43**, 6156–6165 (2015).
- 31) Ruiz-Chica J., Medina M. A., Sánchez-Jiménez F., Ramírez F. J., *Biophys. J.*, **80**, 443–454 (2001).
- 32) Sun C., Tang T., Uludağ H., Cuervo J. E., *Biophys. J.*, **100**, 2754–2763 (2011).
- 33) Matulis D., Rouzina I., Bloomfield V. A., *J. Mol. Biol.*, **296**, 1053–1063 (2000).